

# Realization of wide electron slabs by polarization bulk doping in graded III–V nitride semiconductor alloys

Debdeep Jena,<sup>a)</sup> Sten Heikman, Daniel Green, Dario Buttari, Robert Coffie, Huili Xing, Stacia Keller, Steve DenBaars, James S. Speck, and Umesh K. Mishra  
*Department of Electrical and Computer Engineering and Materials Department, University of California, Santa Barbara, California 93106*

Ioulia Smorchkova  
*TRW, One Space Park R6/1563B, Redondo Beach, California 90277*

(Received 26 April 2002; accepted 8 October 2002)

We present the concept and experimental realization of polarization-induced bulk electron doping in III–V nitride semiconductors. By exploiting the large polarization charges in the III–V nitrides, we are able to create wide slabs of high-density mobile electrons without introducing shallow donors. Transport measurements reveal the superior properties of the polarization-doped electron distributions than comparable shallow donor-doped structures, especially at low temperatures due to the removal of ionized impurity scattering. Such polarization-induced three-dimensional electron slabs can be utilized in a variety of device structures owing to their high conductivity and continuously changing energy gap. © 2002 American Institute of Physics.  
 [DOI: 10.1063/1.1526161]

Doping in semiconductors has been a much researched topic. The traditional shallow “hydrogenic” doping technique is very well understood and gainfully employed. A good understanding of the role of ionized dopant atoms on carrier scattering in semiconductors led to the concept of modulation doping, which improved low temperature carrier mobilities in quantum-confined structures by many orders of magnitude.<sup>1</sup>

The last decade witnessed the emergence of the III–V nitrides as a wide band-gap semiconductor with the property of large embedded electronic polarization fields owing to the lack of inversion symmetry in the crystal structure.<sup>2,3</sup> This property has been widely exploited to make nominally undoped two-dimensional electron gases (2DEGs) in AlGaIn/GaN heterostructures, which had led to high-electron mobility transistors (HEMTs) with record high performance characteristics.<sup>4</sup> The 2DEG at the AlGaIn/GaN interface of a III–V nitride heterostructure is formed to screen the polarization dipole (with spontaneous and piezoelectric contributions) in the thin epitaxial AlGaIn cap layer. Surface donor-like states act as modulation dopants, supplying electrons to form a dipole with the 2DEG at the heterointerface.<sup>5</sup>

The discontinuity of polarization across an  $\text{Al}_x\text{Ga}_{1-x}\text{N}/\text{GaN}$  heterojunction  $\Delta P_{hj} = P_{\text{tot}}^{\text{AlGaIn}}(x) - P_{\text{Sp}}^{\text{GaN}}$  forms a fixed polarization sheet charge at the heterojunction. Grading the AlGaIn/GaN heterojunction over a distance should spread the positive polarization sheet charge into a bulk three-dimensional polarization background charge. The charge profile is given by the divergence of the polarization field, which changes only along the (growth)  $z$  direction [ $N_D^{\text{Pol}}(z) = \nabla \cdot P = \partial P(z)/\partial z$ ]. This fixed charge profile will depend on the nature of the grading; a linear grade results in an approximately uniform profile given by  $N_D^{\text{Pol}}(z)$

$= [P(z_0) - P(0)]/z_0$ . Here  $P(z_0)$  is the polarization (spontaneous + piezoelectric) of  $\text{Al}_x\text{Ga}_{1-x}\text{N}$  at the local Al composition at  $z = z_0$ .

This fixed background charge attracts free carriers from remote donor-like states to satisfy Poisson’s equation and charge neutrality. The end result of the charge rearrangements makes the polarization bulk charge act as a local donor with zero activation energy. The mobile three-dimensional electron slab (3DES) thus formed should be usable just as bulk doped carriers. However, removal of ionized impurity scattering should result in higher mobilities. Such polarization induced electron slabs should in principle be similar to the modulation doped three-dimensional electron slabs in modulation doped wide parabolically graded quantum wells in the AlGaAs/GaAs system.<sup>6</sup> The mobile 3DES should not freeze out at low temperature (as shallow donor doped bulk carriers do), and should exhibit high mobilities at low temperatures. It is noted that we can supply electrons by intentionally introducing a modulation doping layer; we use the surface donors here for convenience. It has been shown that surface donor states are able to supply sheet charges as high as  $n_s = 5 \times 10^{13}/\text{cm}^2$  as demanded by the polarization charge electrostatics;<sup>5</sup> polarization doping as treated in this letter requires surface donors to supply much less carriers than this high value.

To verify these concepts, five samples were grown by molecular beam epitaxy (MBE). Active nitrogen was provided by a rf-plasma source. High resistivity semi-insulating (SI) GaN on sapphire grown by metalorganic chemical vapor deposition (MOCVD) was used as templates. For all five samples, a 100 nm buffer MBE layer of undoped (Ga-face) GaN was grown, followed by a different cap layer for each. The cap layer for the five samples are described in Table I. The top 100 nm of sample 1 is bulk shallow donor doped with Si (activation energy  $E_D = 20$  meV, and concentration  $N_D = 10^{18}/\text{cm}^3$ ). Samples 2, 3, and 4 are linearly graded

<sup>a)</sup>Electronic mail: djena@engineering.ucsb.edu

TABLE I. Sample structures and Hall measurement data for the five samples.

| Sample No. | Cap layer   | Hall sheet density ( $\text{cm}^{-2}$ ) |                      |                      | Hall mobility ( $\text{cm}^2/\text{V s}$ ) |       | 300 K conductivity ( $10^{-4} \Omega^{-1}$ ) |
|------------|---|---|----------------------|----------------------|--|-------|--|
|            |   | Theory                                  | 30 K                 | 300 K                | 30 K                                       | 300 K |  |
| 1          | 100 nm bulk Si doped GaN                                    |   | $7.3 \times 10^{11}$ | $7.0 \times 10^{12}$ | 139  | 329   | 2.3  |
| 2          | 100 nm 0%–10% lin. gr. AlGaIn                               | $2.5 \times 10^{12}$                    | $2.0 \times 10^{12}$ | $1.7 \times 10^{12}$ | 1441                                       | 386   | 0.7  |
| 3          | 100 nm 0%–20% lin. gr. AlGaIn                               | $5.8 \times 10^{12}$                    | $4.9 \times 10^{12}$ | $7.8 \times 10^{12}$ | 2556                                       | 598   | 4.7  |
| 4          | 100 nm 0%–30% lin. gr. AlGaIn                               | $9.0 \times 10^{12}$                    | $9.1 \times 10^{12}$ | $8.9 \times 10^{12}$ | 2605                                       | 715   | 6.4  |
| 5          | 20 nm $\text{Al}_{0.20}\text{Ga}_{0.80}\text{N}/\text{GaN}$ | $7.7 \times 10^{12}$                    | $7.7 \times 10^{12}$ | $7.8 \times 10^{12}$ | 5644                                       | 1206  | 9.4  |

AlGaIn/GaN structures for studying polarization bulk doping; they are graded from GaN to 10%, 20%, and 30% AlGaIn, respectively, over  $z_0 = 100$  nm. Sample 5 is a 20 nm  $\text{Al}_{0.2}\text{Ga}_{0.8}\text{N}/\text{GaN}$  which houses a conventional 2DEG at the heterojunction. Samples 1 and 5 are control samples.

Triple-crystal x-ray diffraction data around the GaN (00.2) peak of samples 1–4 is shown in Fig. 1. The data points match very well with the theoretical solid curves<sup>7</sup> reflecting the high degree of control of Al composition and growth rate in MBE. Atomic force microscopy (AFM) of the sample surfaces revealed step-flow growth and fully strained graded AlGaIn surfaces. Secondary ion mass spectroscopy (SIMS) was performed on an extra graded AlGaIn layer sample specifically grown for that purpose. The linearity of Al composition in the graded layer was revealed by SIMS to be very accurately controlled. It also revealed background oxygen concentration in the MBE GaN layer to be identical to the underlying MOCVD layer accompanied with a small increase in the AlGaIn layers. Any background oxygen [which acts as a shallow donor in (Al)GaN] may provide a small amount of thermally activated carriers which can be frozen out at low temperatures.

Samples were also grown by another growth technique [metalorganic chemical vapor deposition (MOCVD)] and were identical (surface, electrically and structurally) to the MBE grown samples, proving the robustness of the technique of polarization doping. To verify the charge distribution of the 3DES, two samples were grown separately by MOCVD for capacitance–voltage profiling to extract the

spatial charge distribution. The first sample is a 26 nm  $\text{Al}_{0.3}\text{Ga}_{0.7}\text{N}/\text{GaN}$  heterostructure with a 2DEG at the heterojunction, and the second is a graded AlGaIn structure, where the AlGaIn is graded from 0%–10% over a thickness of 100 nm (similar to sample 2). We solved Poisson and Schrödinger equations self-consistently to get the band diagrams and the charge profiles for the two situations. Figure 2 shows the calculated band diagram and the real (zero gate bias) charge profiles for both structures in shaded gray. Polarization coefficients from Ref. 2 were used to simulate the fixed charges. Also shown in the figure are the apparent charge profiles (circles) extracted from a raw  $C-V$  measurement. The apparent carrier profiles in Figs. 2(a) and 2(b) prove that the 2DEG at the heterojunction has been spread out to form a 3DES as a result of the grading. The surface Fermi level causes a partial depletion of the 3DES. A detailed study of the capacitance–voltage profiling technique for reconstruction of the real 3DES profile from the apparent profile using Kroemer's technique<sup>8</sup> for graded heterojunctions will be published as a separate work.

Temperature dependent (20–300 K) Hall measurements were performed on all the five MBE grown samples. Table I shows room temperature and 30 K Hall measurement data for all five samples. The table includes the free carrier density in the bulk GaN and polarization induced 3DES and 2DEG densities calculated by solving Schrödinger and Poisson equations self consistently for samples 2–5. The room temperature sheet conductivity  $\sigma = qn\mu$  is also shown. Temperature dependent carrier densities and mobilities for samples 1, 4, and 5 are plotted in Fig. 3 for comparison. Carriers in the 0%–30% graded AlGaIn sample mimic the transport characteristics of modulation doped 2DEGs and 3DESs characterized by a lack of activation energy, leading to a temperature independent carrier density. Carriers in the bulk donor-doped sample show the characteristic freeze-out associated with the hydrogenic shallow donor nature of Si in bulk GaN. A fit to theoretical dopant activation yielded an activation energy<sup>9</sup>  $E_D = 20$  meV with a doping density (fixed by the Si flux in MBE)  $N_D = 10^{18}/\text{cm}^3$ . The activation energy

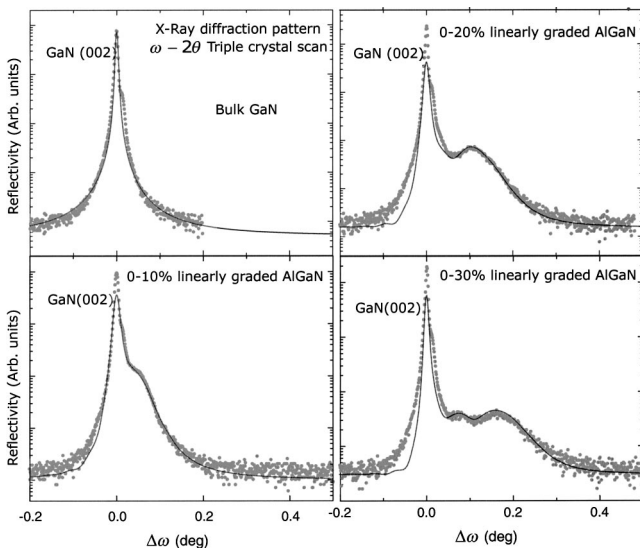


FIG. 1. Triple crystal x-ray diffraction data (dots) and theoretical curve (solid line) for samples 1–4 around the GaN (00.2) peak.

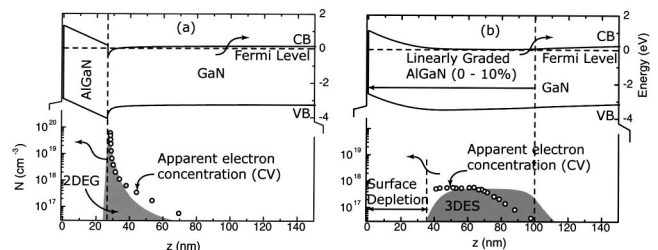


FIG. 2. Band diagram and charge profiles of a 2DEG and a 3DES.

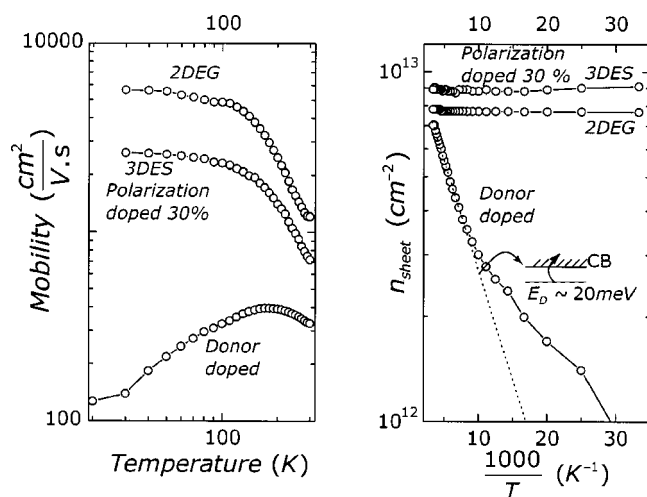


FIG. 3. Temperature dependent carrier sheet densities and mobility for a polarization doped (sample 4), Donor doped (sample 1) and a 2DEG (sample 5) structures.

of Si closely matches that reported by Gotz *et al.*<sup>10</sup> 2DEG carrier mobilities (sample 5) are higher than the shallow donor doped and polarization doped carriers both at room temperature and low temperatures.

The point of interest is more than an order of magnitude improvement of carrier mobility at low temperatures for the polarization doped 3DESs over comparable donor-doped samples. In donor doped GaN, thermally activated carriers freezeout with lowering of temperature leading to less energetic electrons and less effective screening. This causes severe ionized impurity scattering, lowering the mobility. However, the removal of ionized impurity scattering in the polarization doped structure, aided by the complete lack of carrier freezeout at low temperatures results in much improved mobilities. It is not yet clear what limits the low temperature mobility of polarization doped 3DESs. Alloy disorder scattering could be a strong candidate since the 3DES is housed in a linearly graded disordered alloy potential. There is also an improvement of low temperature mobility with increasing carrier density, which points towards possible Coulombic scattering from surface donors, charged dislocations, and background shallow impurities. Dislocation scattering in the polarization doped 3DES is also reduced at low temperatures as compared to donor doped carriers owing to the degenerate nature of 3DES carriers.<sup>11</sup> Scattering from disorder in microscopic dipoles forming the graded alloy polarization charge could also be a source of scattering.<sup>12</sup> The unanswered questions open up avenues for further work in transport of polarization doped 3DESs.

Of special interest to device engineers is the room temperature mobility, and especially the conductivity  $\sigma = en\mu$ . Table I shows that the room temperature charge-mobility product of the polarization doped 3DES (Sample 4) is more than double of that of the comparable donor doped sample (sample 1). Furthermore, the trend with increasing alloy composition suggests that the conductivity increases with increasing carrier density (got by either grading to higher aluminum composition for the same thickness, or decreasing the thickness for same grading composition). This trend is very

useful for the design of high conductivity layers required in many device structures, especially in field effect transistors (FETs) and regrown ohmic contacts. The additional band discontinuity achieved at a regrown polarization-doped AlGaIn ohmic contact will serve as an efficient hot-electron launcher from the source into the FET channel, reducing transit times. The flexibility of polarization doping by grading (by controlling alloy composition and/or graded layer thickness independently) is an added attraction. An interesting extension is the possibility of achieving polarization doped *p*-type carriers with higher mobilities by grading down from AlGaIn for Ga-face III-V nitrides (or grading up from GaN to AlGaIn in *N*-face III-V nitrides). In such polarization doped 3D hole slabs (3DHS), one might need to supply holes through remote acceptors. The might solve the problems associated with the high activation energy of the commonly used acceptor (Mg) for GaN. Our work presents the first step towards realizing the proposed enhancement of base conductivity in AlGaIn/GaN heterojunction bipolar transistors by exploiting the strong electronic polarization properties of the III-V nitride semiconductors.<sup>13</sup> Finally, an important outcome of the work in device design would be the requirement of compensation doping in graded III-V (Al)GaIn layers for removing unwanted mobile carriers that will necessarily result from polarization doping.

In conclusion, we have demonstrated that polarization fields can be engineered to achieve bulk doping as an attractive alternate doping technique in III-V nitride semiconductors. We demonstrate improved conductivity of polarization-doped layers over comparable donor-doped layers, and point out avenues where it may be gainfully employed.

The authors would like to thank Patrick Waltereit, Arthur C. Gossard, and Herbert Kroemer for useful discussions. Funding from POLARIS/MURI (Contract monitor: C. Wood) is gratefully acknowledged.

<sup>1</sup>L. Pfeiffer, K. W. West, H. L. Stormer, and K. W. Baldwin, Appl. Phys. Lett. **55**, 1888 (1989).

<sup>2</sup>F. Bernardini, V. Fiorentini, and D. Vanderbilt, Phys. Rev. B **56**, R10024 (1997).

<sup>3</sup>P. Waltereit, O. Brandt, A. Trampert, H. T. Grahn, J. Menniger, M. Ramsteiner, M. Reiche, and K. H. Ploog, Nature (London) **406**, 865 (2000).

<sup>4</sup>Y. F. Wu, B. P. Keller, P. Fini, S. Keller, T. J. Jenkins, L. T. Kehias, S. P. Denbars, and U. K. Mishra, IEEE Electron Device Lett. **19**, 50 (1998).

<sup>5</sup>J. P. Ibbetson, P. T. Fini, K. D. Ness, S. P. Denbars, J. S. Speck, and U. K. Mishra, Appl. Phys. Lett. **77**, 250 (2000).

<sup>6</sup>M. Shayegan, T. Sajoto, M. Santos, and C. Silvestre, Appl. Phys. Lett. **53**, 791 (1988).

<sup>7</sup>O. Brandt, P. Waltereit, and K. Ploog, J. Phys. D **35**, 577 (2002).

<sup>8</sup>H. Kroemer, W. Y. Chien, J. S. Harris, Jr., and D. D. Edwall, Appl. Phys. Lett. **36**, 295 (1980).

<sup>9</sup>We corrected the transport measurement of the bulk sample since it revealed a degenerate layer below 30 K using the two-layer model developed for GaN bulk layers; see D. C. Look and R. J. Molnar, Appl. Phys. Lett. **70**, 3377 (1997).

<sup>10</sup>W. Götz, N. M. Johnson, C. Chen, H. Liu, C. Kuo, and W. Imler, Appl. Phys. Lett. **68**, 3144 (1996).

<sup>11</sup>D. Jena, A. C. Gossard, and U. K. Mishra, Appl. Phys. Lett. **76**, 1707 (2000).

<sup>12</sup>D. Jena, A. C. Gossard, and U. K. Mishra, J. Appl. Phys. **88**, 4734 (2000).

<sup>13</sup>P. M. Asbeck, E. T. Yu, S. S. Lau, W. Sun, X. Dang, and C. Shi, Solid-State Electron. **44**, 211 (2000).